

Subsurface warming derived by Argo floats during the 2022

Mediterranean marine heatwave

Annunziata Pirro¹, Riccardo Martellucci¹, Antonella Gallo¹, Elisabeth Kubin¹, Elena Mauri¹, Mélanie Juza², Giulio Notarstefano¹, Massimo Pacciaroni¹, Antonio Bussani¹, Milena Menna¹

¹National Institute of Oceanography and Applied Geophysics (OGS), Trieste, 34010, Italy

²Laboratory Balearic Islands Coastal Observing and Forecasting System (SOCIB), Palma, 07122, Spain

Correspondence to: Annunziata Pirro (apirro@ogs.it)

Abstract.

The Mediterranean marine heatwave (MHW) during the warm season (May-September) and the fall period (October-December) of 2022 is analyzed using Argo float in-situ observations in the upper 2000 m of depth. Five study regions (North Western Mediterranean, South Western Mediterranean, central Ionian Sea, Pelops Gyre and southern Adriatic Sea) most affected by warming in different layers were selected and investigated. Temperature anomaly profiles $T_a(z)$ computed for each area and for both periods were divided into three categories based on vertical heat penetration: Category 1 (shallow, 0-150 m), Category 2 (intermediate, 150-700 m) and Category 3 (deep, > 700 m). During the warm season, Category 1 profiles had a temperature anomaly near zero or slightly negative in a thin layer between 50 m and 150 m depth, while warming was observed in the 0-50 m layer and below the middle layer. Profiles characterized by greater vertical heat penetration (categories 2 and 3) were mainly in mesoscale or sub basin structures and showed the largest positive temperature anomaly in the surface **and intermediate layers**. All profile categories showed a warming between 200 and 800 m depth. This increase is roughly split, with half attributed to the impact of the 2022 MHW, and the other half linked to the ongoing long-term trend in ocean temperatures. During the fall period **and in the layer below 200 m depth, the shape of the temperature anomaly profiles are similar for all sectors with the exception of the South Adriatic Pit, which depict a +0.5° C warming at 800 m depth.**

The present work highlights the warming characteristics along the entire water column in different regions of the Mediterranean Sea, some of which are characterized by dynamic activities (e.g. dense water formation, upwelling) therefore, **any variation of the associated ocean processes can have implication on the thermohaline circulation and thus, on the climate system.**

30 Introduction

31 Marine heatwaves (MHWs) are extreme ocean temperature events occurring over extended periods of time (Hobday et al.,
32 2016). Over the past decade **the frequency of MHW events has increased by 50%** (IPCC, 2023) as well as their duration and
33 magnitude (Oliver et al., 2018). They can affect small areas of coastline or span multiple ocean areas across latitudes with
34 significant impacts on ecosystems, coastal communities and economies (Wernberg et al., 2013; Garrabou et al., 2022; Dayan
35 et al., 2023).

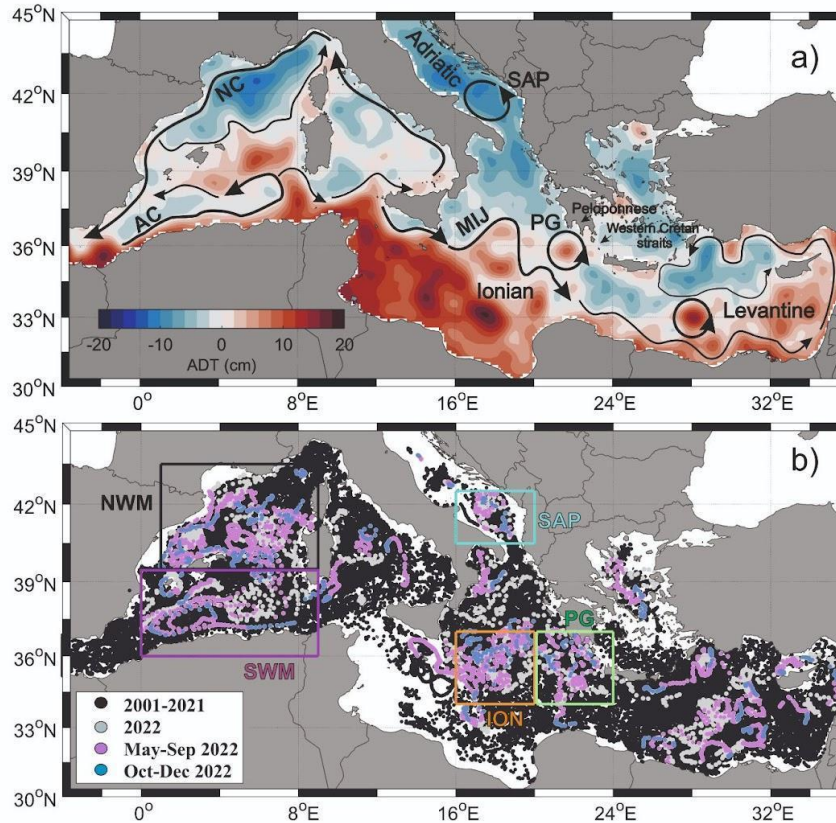
36 **Since the beginning of the 21st century the particularly rapid warming trend of the Mediterranean Sea surface layer has been**
37 **associated with a strong increase in MHWs events** (Bensoussan et al., 2019, Ibrahim et al, 2021, Juza et al., 2022, Pastor and
38 Khodayar, 2022, Dayan et al., 2023). Several studies, mainly confined at the surface, have addressed this topic **covering**
39 **different aspects of MHWs using satellite observations and model simulations.** In particular, from basin to sub-regional scale,
40 previous works **analyze** MHWs drivers and indicators, estimate the frequency, the duration and intensity of MHWs, evaluate
41 their trend and assess the risk and the impacts on ecosystems (Darmaraki et al 2019, Galli et al., 2017, Garrabou et al., 2022,
42 Juza et al., 2022, **Dayan et al., 2023, Martinez et al., 2023, Marullo et al., 2023, Pastor and Khodayar, Simon et al., 2023**).

43
44 However, MHWs are not exclusively limited to the surface layer, but they can also propagate throughout the deeper layers of
45 the water column (Darmaraki et al., 2019, Shijian et al., 2021, Scannell H.A., 2020, Juza et al., 2022). **This can cause negative**
46 **ecological consequences compromising the maintenance of the biodiversity, of the food and the regulation of air quality**
47 **(Garrabou et al., 2022; Holbrook et al., 2020; Santora et al., 2020; Smale et al., 2019; Schaeffer and Roughan, 2017; Liquete**
48 **et al., 2016; Martín-Lopez et al., 2016; Mills et al., 2013).** A recent work in the Mediterranean Sea shows that although
49 MHWs frequency is higher at the surface, their maximum intensity and duration is registered in the subsurface layers (Dayan
50 et al., 2023). Moreover, in-situ data collected in the tropical western Pacific Ocean show that the maximum intensity of almost
51 every MHW event is found in the subsurface layer, and many of the MHWs occurred even when no significant warming
52 anomalies are detected at the surface (Shijian et al., 2021).

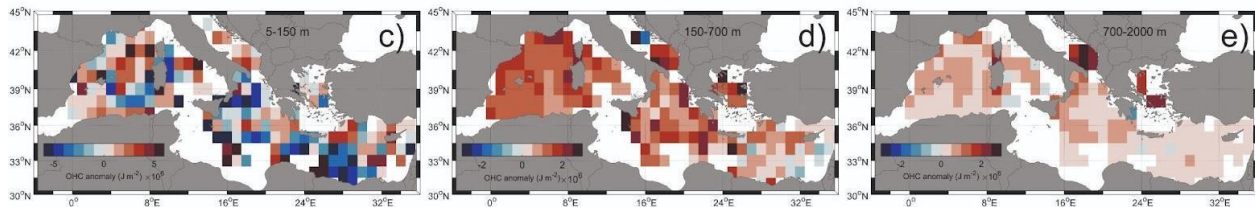
53
54 **Using satellite data, Marullo et al. (2023) defined the occurrence of the event in the Mediterranean Sea from May 2022 to**
55 **spring 2023, with higher intensity in summer 2022 and in the band 0-25° E. Starting from this result, the present work**
56 **analyzes the subsurface properties of the 2022 MHW in the upper 2000 m depth using in-situ hydrographic Argo profiles**
57 **(Product ref. no. 1, Table 1; Wong et al., 2020) collected during the period of highest intensity (warm season, May-**
58 **September) and in the period thereafter (cold season, October-December) . Focusing on Marullo et al. (2023) results and**
59 **on the availability of Argo float profiles, five study areas were selected for our analysis (Figure 1(b)). An estimation of the**
60 **horizontal and vertical distribution of the Ocean Heat Content (OHC) anomaly is performed in the whole Mediterranean.**
61

Product ref. no.	Product ID & type	Data access	Documentation
1	INSITU_MED_PHYBGCWAV_DISCRETE_MYNRT_013_035; In-situ observations	EU Copernicus Marine Service Product, 2022a;	Quality Information Document (QUID): Wehde et al., (2022) Product User Manual (PUM): In Situ TAC partners (2022)
2	MEDSEA_MULTIYEAR_PHY_006_004; numerical models	EU Copernicus Marine Service Product, 2022b;	Quality Information Document (QUID): Escudier al., (2022) Product User Manual (PUM): Lecci et al., (2022)
3	SEALEVEL_EUR_PHY_L4_NRT_OBSERVATIONS_008_060; satellite observations	EU Copernicus Marine Service Product, 2023;	Quality Information Document (QUID): Pujol al., (2023) Product User Manual (PUM): Pujol., (2022a)
4	SEADATANET_MedSea_climatology_V2; climatology	SEADATANET Product; 2022	Product Information Document (PIDoc): Simoncelli et al. (2020)

62 **Table 1: Product data used to perform the analysis of the present work**



64



65 **Figure1: (a) Absolute Dynamic Topography (colours) averaged from spring-summer (May-September 2022) along with schematic**
 66 **pathways (black arrows) of the Algerian Current (AC), Northern Current (NC), Mid-Ionian Jet (MIJ), South Adriatic Pit (SAP)**
 67 **and Pelops Gyre (PG). (b) Argo floats position for the whole Mediterranean Sea. Black, magenta, cyan, orange and green boxes**
 68 **indicate the North West Mediterranean (NWM, 39.5-43.5°N; 1-9°E), South West Mediterranean (SWM, 36-39.5°N; 0-9°E), South**
 69 **Adriatic Pit (SAP, 40.5-42.5°N; 16-20°E), Ionian (ION, 34-37°N; 13-20°E) and Pelops Gyre (PG, 34-37°N; 20-24°E) areas,**
 70 **respectively. (c-e) 2022 Ocean Heat Content (OHC) anomaly estimated with respect to the 2001-2018 FLOAT climatology period**
 71 **from Argo floats profiles in different layers (c, 5-150m), (d, 150-700), (e, 700-2000).**

72 Based on the vertical heat penetration (MHW depth, see Methods section), the **temperature profiles collected in May-**
 73 **September 2022** from each study area were divided into three categories (shallow, intermediate and deep penetration) and the

74 mean profile of temperature anomaly (T_a) was computed for each of them. Changes in the vertical temperature anomalies were
75 described and analyzed in relation to the ocean stratification, circulation and dynamics of each specific area. Lastly, this study
76 examines the properties of the water column during the fall period and speculates on its relationship with the dynamics of the
77 previous warm season's MHW. An estimation of the horizontal and vertical distribution of the Ocean Heat Content (OHC)
78 anomaly in 2022 was also performed in the whole Mediterranean Sea.
79

80 **Methods**

81 The vertical propagation of the 2022 MHW in the Mediterranean Sea was investigated using temperature data collected by
82 Argo floats in the period 2001-2022 (Figure 1(b)). These data were collected and made freely available by the International
83 Argo Program (which is part of the Global Ocean Observing System (Argo 2023)) and by the national program Argo Italy that
84 contributes to it (<https://argo.ucsd.edu>, last access 23 April 2023; <https://www.ocean-ops.org>, last access 23 April 2023).
85).

86 A comprehensive characterization of the event over the whole Mediterranean Sea was performed starting from the OHC
87 analysis. The OHC, defined as the total amount of heat absorbed and stored by the ocean, can be considered as a good indicator
88 for assessing the Earth's energy imbalance (Von Schuckmann et al., 2016). A float derived OHC climatology (OHC₂₀₀₁₋₂₀₁₈)
89 for the period 2001-2018 was estimated in 1° x 1° bins and in different layers (0-150 m, 150-700 m, 700-2000 m) using the
90 method of Kubin et al., 2023. Subsequently, Argo temperature data collected in 2022 were averaged on the same grid of
91 OHC₂₀₀₁₋₂₀₁₈ to compute the 2022 OHC (OHC₂₀₂₂). The OHCA₂₀₂₂ was then calculated as the difference between OHC₂₀₂₂ and
92 OHC₂₀₀₁₋₂₀₁₈ fields.

93 The five Mediterranean Sea regions most affected by surface warming (Figure 1b) were selected using the results of Marullo
94 et al. (2023) and considering the availability of float data. In these regions we analyzed the vertical penetration of the 2022
95 MHW signal in the water column both during the warm and cold season. The regions selected are: the North Western
96 Mediterranean (NWM), the South Western Mediterranean (SWM), the Ionian (ION), the Southern Adriatic Pit (SAP) and the
97 Pelops Gyre (PG) sectors.

98 The Temperature anomaly T_a at each depth z and for each profile was computed as:

$$T_a(z) = T(z) - \underline{T}(z), \quad (1)$$

99 for each sector. $T(z)$ is the 2022 temperature derived from Argo floats while $\underline{T}(z)$ is the climatological (1985-2018) averaged
100 temperature derived from the SeaDataCloud dataset (Product ref. no. 4, Table 1; SDC climatology). Specifically, the gridded
101 (0.125° x 0.125°) monthly climatological profiles were linearly interpolated in depth (every 10 m) and at the position of each

102 float profile. Moreover, to compare the 2022 MHW event with the averaged conditions estimated by floats in the selected
 103 sectors, T_a profiles were also computed for the whole float dataset in the period 2001-2018 (FLOAT climatology). **It's important**
 104 **to highlight that while this study utilizes the SDC climatology, the FLOAT climatology was utilized to facilitate a**
 105 **straightforward comparison with the OHC findings from Kubin et al., 2023.** The time window used for the present work (May-
 106 September 2022) was chosen based on the latest European Space Agency specification
 107 (https://www.esa.int/Applications/Observing_the_Earth/Mediterranean_Sea_hit_by_marine_heatwave, last access 18
 108 February 2023) and on the estimations of Marullo et al. (2023). **These indicate that** the 2022 MHW developed in the second
 109 half of April in the northwest Mediterranean Sea and extended over the central Mediterranean into September. In this period,
 110 T_a profiles were quality controlled to remove any inconsistency (e.g. profiles with negative surface anomalies) and used to
 111 estimate the vertical propagation of the MHW (or MHW depth), following the method of Elzahaby and Schaeffer 2019. For
 112 each profile, the positive threshold depth (hereafter Z_N) is defined as the depth at which the first negative or 0 temperature
 113 anomaly occurred:

$$Z_N = \min (z(T(z) \leq 0)), \quad (2)$$

114 Knowing Z_N , the vertical cumulative temperature anomaly (CT_a) defined as:

$$CT_a(Z_N) = \sum_{z=0}^{Z_N} T(z) \Delta z, \quad (3)$$

115 with $\Delta z = 10$ m, was computed for each profile from the surface ($z=0$) to the positive
 116 threshold depth ($z=Z_N$). To reduce the effect of the insignificant warming at depths per water profile, we define the
 117 MHW depth as the depth where a fraction ($\varepsilon=0.95$) of the cumulative T_a is reached:

$$MHWdepth = \max (z(CT_a(z) \leq \varepsilon \cdot CT_a(Z_N))), \quad (4)$$

118 Based on MHW depth values, T_a profiles were then divided into three categories: Category 1 (shallow, 0-150 m), Category 2
 119 (intermediate, 150-700 m) and Category 3 (deep, > 700 m). **It's noteworthy that within the SAP area, floats categorized as**
 120 **Category 2 and Category 3 consistently exhibit no negative temperature anomalies. However, they are classified into these**
 121 **categories based on their respective depths—shallower or deeper than 700 meters. Additionally, despite the limited number of**
 122 **profiles available in this region, they all fall within the cyclonic gyre. Hence, we are confident in considering them as**
 123 **representative of the entire SAP region.** The median profile (\bar{T}_a) for each category was obtained by spatially averaging all the
 124 available data in the different sectors in the spring-summer period using both 2022 and FLOAT climatology Argo
 125 data. **Considering that the 2022 MHW extends until the spring of 2023, (Marullo et al., 2023), the median profiles \bar{T}_a for the**
 126 **fall period \bar{T}_a were also examined to investigate the accumulation of the heat in the water column . The mean T_a averaged in**

127 the surface, intermediate and deep layers as well as other additional information (number of profiles, MHW depth, max T_a and
 128 depth of max) are listed in Table 2.

129 Lastly, the Brunt-Väisälä frequency squared (N^2) for the year 2022 and in the upper 150 m depth was computed using **monthly**
 130 **averaged temperature and salinity Argo floats profiles for each sector in order to characterize the vertical heat penetration**. The
 131 same procedure was adopted to calculate the N^2 anomaly with respect to FLOAT climatology.

			Number of profiles	MHW depth (m)	T anomaly (°C)			Mean T anomaly (°C)		
					at the surface (10 m)	Max	Depth of Max (m)	0-150 m	150-700 m	700- 2000 m
NWM	spring summer	C1	335	24.8	2.3	5.82	22.5	0.28	0.32	0.097
		C2	16	571.9	2.2	5.48	50	0.32	0.4	NaN
		C3	43	1457.9	2.92	5.58	19.5	0.8	0.36	0.1
		clim	2460	-	-	-	-	0.12	0.06	0.025
	fall	2022	306	-	-	-	-	0.66	0.33	0.11
		clim	1284	-	-	-	-	0.08	0.07	0.04
SWM	spring summer	C1	159	25.6	2.13	5.79	22.5	0.19	0.33	0.088
		C2	5	630	1.83	5.46	24	0.43	0.3	NaN
		C3	27	1409.6	2.24	5.05	24.1	0.86	0.36	0.095
		clim	2168	-	-	-	-	0.028	0.059	0.028
	fall	2022	148	-	-	-	-	0.18	0.31	0.11
		clim	1456	-	-	-	-	0.1	0.05	0.02
ION	spring summer	C1	105	22.8	1.34	4.58	22.2	0.03	0.27	0.12
		C2	5	644	2.18	2.87	18	0.58	0.35	0.54
		C3	3	1383.4	1.39	1.97	20	0.47	0.54	0.15
		clim	1148	-	-	-	-	0.071	0.091	0.057
	fall	2022	119	-	-	-	-	-0.21	0.26	0.12
		clim	695	-	-	-	-	-0.06	0.07	0.05
PG	spring summer	C1	50	37	1.34	3.82	41	0.15	0.32	0.03
		C2	15	553.4	0.95	6.15	47.3	0.97	0.34	0
		C3	20	1043.5	0.88	5.34	40	1.14	0.58	0.05
		clim	1073	-	-	-	-	0.3	0.15	0.02
	fall	2022	70	-	-	-	-	-0.2	0.19	-0.02
		clim	590	-	-	-	-	0.27	0.13	0
SAP	spring summer	C1	9	32.2	1.18	3	24.5	0.57	0.39	0.66
		C2	10	411	1.95	7.25	27	1.04	0.46	NaN
		C3	17	945.3	0.88	4.36	78.8	0.72	0.4	0.59
		clim	619	-	-	-	-	0.3	0.21	0.21
	fall	2022	44	-	-	-	-	0.27	0.41	0.69
		clim	372	-	-	-	-	0.29	0.2	0.16

132

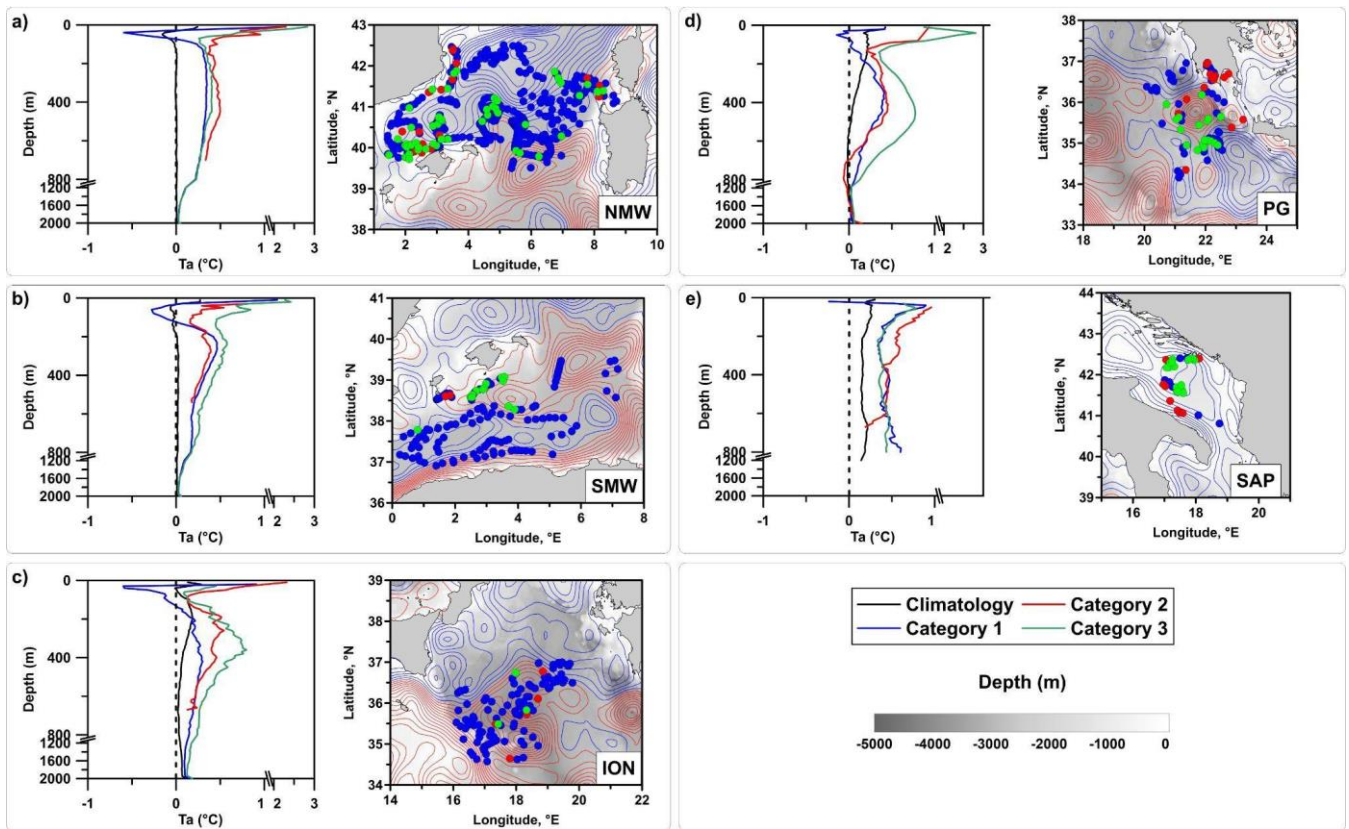
133 **Table 2: Characteristics of the 2022 MHW in Category 1(C1), Category 2 (C2), Category 3 (C3): MHW depth, surface temperature**
 134 **anomaly (Surface), maximum temperature anomaly (Max) and the depth where it occurs (Depth of max), mean temperature**

135 anomaly for the surface (0-150 m), intermediate (150-700 m) and deep (700-2000 m) layers for each category and for the FLOAT
136 Climatology (clim).

137

138 **Results and discussion**

139 In the surface layer, the OHCA₂₀₂₂ displayed inhomogeneous warming patterns, with positive anomalies areas adjacent to
140 others with strong negative anomalies (Figure 1(c)). Largest positive anomalies were observed in the West Mediterranean, in
141 the South Adriatic, in the eastern Ionian and northern Levantine basin. In the intermediate and deep layers the warming was
142 more homogeneous and widespread i (Figures 1(d), 1(e)) where the majority of bins showed positive values of the OHCA₂₀₂₂
143 and specifically, the western and central Mediterranean areas along with the Aegean Sea showed a more pronounced warming
144 compared to the Levantine basin, which exhibits a slight cooling in some bins of the central and eastern sectors. It can be stated
145 that half of this warming in the intermediate and deep layers is due to the 2022 MHW while the other half to the long-term
146 warming of the ocean. This consideration stems from comparing the current OHCA₂₀₂₂ with OHC trends defined by Kubin
147 et al. (2023) To perform this study, five regions (NWM, SWM, ION, SAP and PG; coloured boxes in Figure 1(b)) were
148 selected. This choice was motivated by the highest 2022 SST anomaly registered in the band 0 - 25° E (Marullo et al. 2023)
149 and by the availability of float data in both May-September and October-December 2022 periods. Figure 2 shows T_a profiles
150 for the warm season of each sector, for each MHW depth category and for the FLOAT climatology.



151

152

153

154 **Figure 2: (left panels) Median profiles of temperature anomaly computed for each sector (NWM, SWM, ION, PG, SAP) and for the**
 155 **2022 warm season (May-September) using Argo floats data with respect to the 1985-2018 SDC climatology dataset. Black lines**
 156 **highlight the FLOAT climatology profiles while blue, red and green profiles indicate shallow (0-150 m), intermediate (150-700 m)**
 157 **and deep (> 700m) categories, respectively. (right panels) Positive and negative contours of the Absolute Dynamic Topography with**
 158 **1 cm spacing are displayed by red and blue lines while the coloured dots are associated to the floats position of each category.**

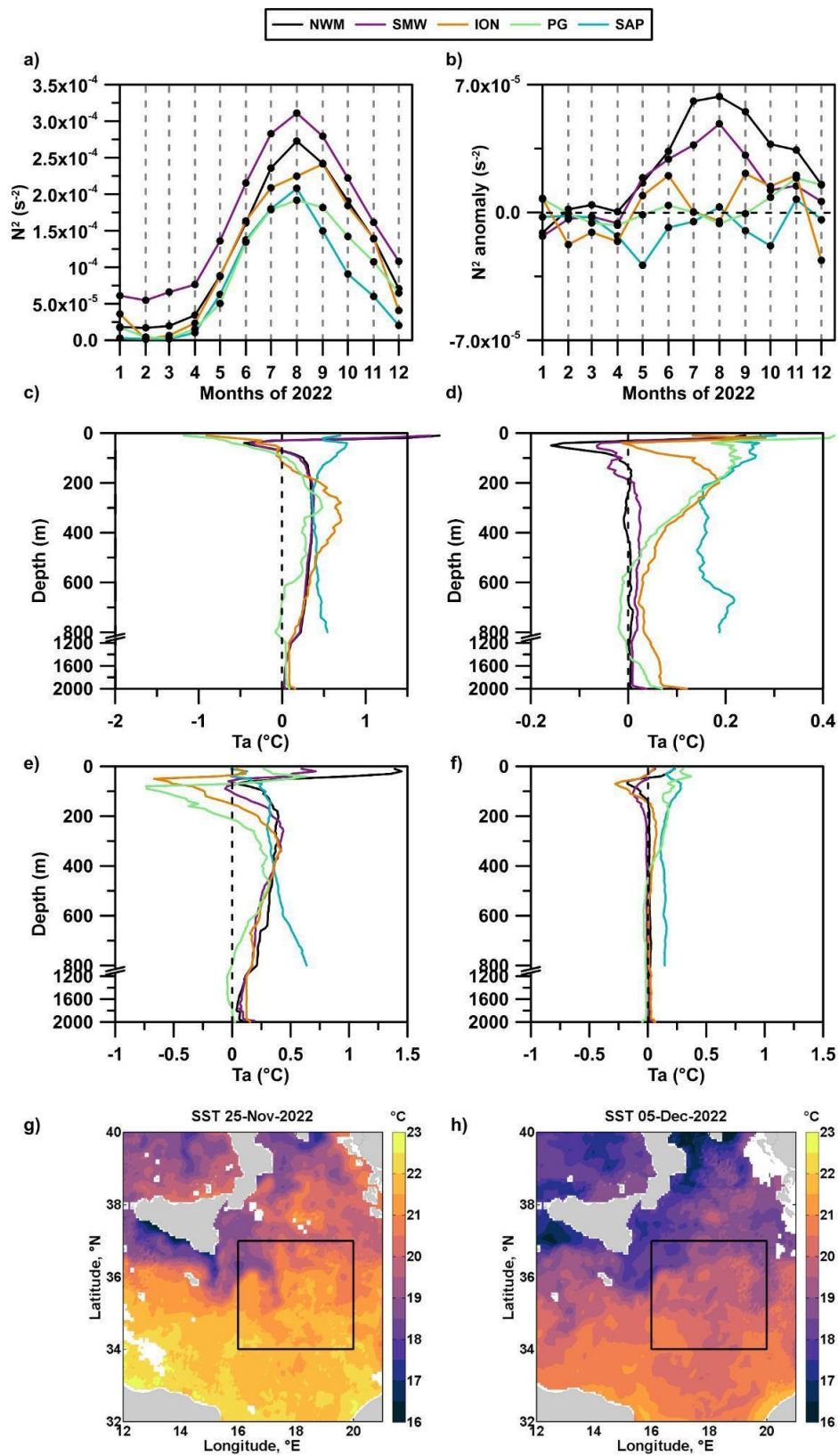
159 **In the NWM and SWM sectors the circulation is strongly influenced by the presence of two intense and permanent currents**
 160 **(Figure 1(a)): the south-westward Northern Current (Poulain et al., 2012; Escudier et al., 2021) and the eastward along-slope**
 161 **Algerian Current (which transports waters of Atlantic origin in the upper water column (Poulain et al., 2021)) in the NWM**
 162 **and in the SWM, respectively. Therefore, float profiles were mainly located along the boundary of cyclonic circuits as**
 163 **highlighted by the Absolute Dynamic Topography (Product ref. no. 3, Table 1; (Figures 2(a), 2(b))). In the ION sector, float**
 164 **profiles were mainly distributed in the anticyclonic meander of the Mid-Ionian Jet (Figure 2(c)), a strong meandering current**
 165 **that together with the Atlantic-Ionian Stream (AIS), transports Atlantic Water from the western to the eastern Mediterranean**

166 Sea (Poulain et al., 2012, 2013; Menna et al., 2019a; Figure 1(a)). Although the NWM, SWM and ION sectors have different
167 oceanographic characteristics, they showed a similar response to the 2022 MHW (Figure 2(a-c)). Most $\underline{T}a_{(TOGLI\ LINEA)}$ profiles
168 belong to Category 1 and the mean MHW depth falls into the 20-25 m layer (Table 2). Profiles, characterized by shallow
169 MHW penetration (blue lines in Figures 2(a-c)), showed decreasing warming in the first 50 m with the maximum $\underline{T}a_{(TOGLI\ LINEA)}$
170 close to the surface (22.2-22.5 m; Table 2). The layer between 50 and 100 m depth showed a negative $\underline{T}a$ with maxima
171 of -0.6°C , -0.3°C and -0.6°C at 40 m, 70 m and 30 m depth, in the NWM, SWM and ION sectors, respectively. The median
172 profiles derived from the FLOAT climatology (black lines in Figure 2(a-c)) do not exhibit this negative anomaly (or only to
173 a very small extent), suggesting, therefore, a possible link between this behavior and the occurrence of the 2022 MHW. Below
174 100 m depth, the $\underline{T}a$ becomes positive again with mean values of $\sim 0.3^\circ\text{C}$ in the intermediate layer and values lower than 0.12°C
175 in the deep layer. Profiles characterized by intermediate MHW penetration (red lines in Figures 2(a-c); MHW depth between
176 570 m and 650 m, Table 2) were located in coastal areas of the Western Mediterranean and in frontal zones in the ION sector,
177 and showed positive $\underline{T}a$ throughout the water column, with values in the range of $0.3 - 0.6^\circ\text{C}$. Profiles, characterized by deep
178 MHW penetration (green lines in Figures 2(a-c); MHW depth ~ 1400 m, Table 2), showed the largest $\underline{T}a$ in the surface
179 layer in the two sectors of the West Mediterranean ($> 2^\circ\text{C}$), while the ION sector depicted
180 the largest anomalies in the intermediate layer ($> 0.8^\circ\text{C}$). These results are consistent with
181 the warming trend of the Western Mediterranean Sea over the last 15 years of 0.09 ± 0.02
182 $(0.03\pm 0.01)^\circ\text{C}\cdot\text{yr}^{-1}$ for surface (intermediate) waters (Kubin et al., 2023).

183 The PG is located on the eastern side of the northern Ionian Sea, southwest of the Peloponnese coast (Figure 1(a)). It is a sub-
184 basin anticyclonic feature (diameter of ~ 120 km; Pinardi et al., 2015) which extends from the surface down to 800-1000 m
185 depth (Malanotte-Rizzoli et al., 1997; Kovacevic et al., 2015) and it is forced by the Etesian winds (Ayoub et al., 1998;
186 Mkhinini et al., 2014; Menna et al., 2021). In the late summer/fall the Etesian winds amplify their acceleration and the wind
187 shear in the region of the western Cretan straits (Mkhinini et al., 2014) therefore, larger anticyclonic vorticities are observed
188 during these months in the surface layer of the PG region (Menna et al., 2019a). In the sector PG, $\underline{T}a$ profiles for the three
189 categories showed positive temperature anomalies in the first 800 m of the water column which coincides with the vertical
190 extension of the gyre itself (Figure 2(d)). Profiles that fall into Category 1 showed decreasing warming in the first 70 m,
191 anomaly values close to zero in the 70-150 m layer and increasing warming in the 150-400 m layer. The mean anomaly in the
192 intermediate layer of Category 1 is 0.3°C (Table 2). Category 2 profiles were retrieved mainly in the coastal area near the
193 Peloponnese while Category 3 profiles were found within the gyre area. Categories 2 and 3 showed strong warming in the
194 surface layer (0.97°C and 1.14°C , respectively), a mean warming in the range of $0.3-0.6^\circ\text{C}$ in the intermediate layer and no
195 warming compared to the SDC climatology was observed in the deep layer (Table 2).

196 The SAP is one of the sites of open ocean convection in the Mediterranean Sea, characterised by a complex thermohaline
197 circulation that influences the physical and biogeochemical properties of the dense waters formed in its interior and the strength
198 of winter convection (Menna et al., 2022 OSR6; Pirro et al., 2022; Di Biagio et al., 2023). This sector showed positive
199 temperature anomalies in all layers and in all categories (Figure 2(d)). Most profiles belong to Category 3 with a mean MHW
200 depth of ~ 950 m and maximum T_a at ~ 80 m depth. The largest mean warming was observed in the surface layer of each
201 category (0.6 - 1.04° C) followed by the deep layer, which had an exceptional warming of $\sim 0.6^\circ$ C, and finally by the
202 intermediate layer, with a mean warming of $\sim 0.4^\circ$ C (Table 2).

203 All five sectors showed a larger warming than the FLOAT climatology with a mean temperature increase in spring-summer
204 2022 between 0.2° C and 0.8° C in response to the MHW event (Table 2). Some differences in warming observed among the
205 sectors are related to their peculiar hydrological and dynamical characteristics. During the spring-summer period, the surface
206 layer of the NWM and SWM sectors and partially of the ION sector, was characterized by both larger stratifications and
207 stratification anomalies compared to the FLOAT climatology (Figures 3(a), 3(b)). Strong stratification prevents vertical heat
208 penetration causing negative T_a in the 50-100 m layer (Figure 2(a-c)). In the PG sector, summer-spring stratification anomaly
209 was consistent with climatology (Figure 3(b)), and vertical heat penetration was closely related to the gyre dynamics. In the
210 SAP sector, stratification during the summer-spring period was lower than climatology suggesting an instability of the water
211 column and therefore the transport of the vertical heat to the deep layers. The median of all profiles available in spring-summer
212 2022, when not categorized, closely aligns with the median of profiles in category C1 (Figures 3(c), 3(d)). This condition arises
213 because category C1 consistently boasts the highest number of profiles across various sectors.



215 **Figure3: (a) Monthly averaged Brunt - Väisälä frequency squared (N^2) computed in the surface layer (0-150 m) using 2022 Argo**
216 **float data. (b) Monthly averaged Brunt Brunt—Väisälä frequency squared anomaly (N^2 anomaly) computed in the surface layer**
217 **with respect to the FLOAT climatology. (c) Median Temperature anomaly ($^{\circ}\text{C}$) computed in the warm season (May - September)**
218 **from Argo floats profiles in 2022 and (d) in 2001-2018 with respect to the SDC climatology. (e) Median Temperature anomaly ($^{\circ}\text{C}$)**
219 **computed in fall period (October - December) from Argo floats profiles in 2022 and (e) in 2001-2018 with respect to the SDC**
220 **climatology). (g) Daily Sea Surface Temperature ($^{\circ}\text{C}$) in the ION sector (black box) for late November and (h) early December**
221 **2022.**

222 Larger warming of the water column was observed in fall 2022 compared to the SDC climatology in all sectors, except for the
223 surface layer of the ION and PG sectors (Figure 3e). The stronger spring-summer stratification observed in the NWM and
224 SWM sectors (Figures 3(a), 3(b)) corresponds to enhanced vertical heat propagation in the surface and intermediate layers in
225 fall 2022 (Figure 3(e), Table 2). Negative T_a values in the surface layer of the ION sector were attributed to an upwelling event
226 along the southern coast of Sicily between November and December 2022 as shown by the Sea Surface Temperature (Product
227 ref. no. 2, Table 1; (Figures 3(g), 3(h)). The northern part of the Sicily Channel is an area of strong eddy kinetic energy (Poulain
228 et al., 2012) influenced by Ekman transport and advection of waters from the western to the eastern Mediterranean (Molcard
229 et al., 2002; Falcini et al., 2015; Schroeder et al., 2017; Menna et al., 2019b). The cold waters upwelled off the southern coast
230 of Sicily in November 2022 (Figure 3(g)) were advected to the Ionian Sea through the Atlantic-Ionian Stream and the Mid-
231 Ionian Jet pathways (Figure 1(a)), and gradually cooling the waters in the ION sector (Figure 3(h)). The negative anomaly in
232 the surface layer of the ION sector is not limited only to 2022 but is a permanent characteristic of the area related to the
233 upwelling phenomena, as confirmed by the T_a profile derived from the FLOAT climatology (orange line in Figure 3(f)) and
234 by trends of the OHC anomaly estimated by Dayan et al. (2023) over the period 1987-2019. Negative T_a values in the PG
235 sector were imputable to the typical downwelling process of this region associated with the gyre dynamics. The downwelling
236 contributed to the vertical propagation of the 2022 MHW, with a strong spring-summer warming in the first 800 m of the water
237 column (Figure 2d), keeping the stratification values similar to the FLOAT climatology (no significant increases of N^2 anomaly
238 was registered due to the 2022 heatwave; Figure 3(b)). In this way, fall cooling can penetrate deep into the water column
239 causing, therefore, negative T_a values in the surface layer (Figure 3(e); Table 2).

240 In recent years, the SAP is experiencing a significant temperature increase in the deep layer (trend of $\sim 0.06^{\circ}\text{C}\cdot\text{yr}^{-1}$ in the
241 2013-2020 period according to Kubin et al., 2023) and salinity in the surface and intermediate layers (Mihanovich et al., 2021;
242 Menna et al., 2022 OSR6) with potential future effects on the whole thermohaline cell of the Eastern Mediterranean. It is of
243 general understanding that convection sites contribute to the propagation of the MHWs signal from the surface to the
244 subsurface interior of the water column (Dayan et al., 2023; Kubin et al., 2023) but specific analysis at the local scale are not
245 yet available (Juza et al., 2022). Our results show a fair significant warming of the SAP in both spring summer (Figure 2(e))
246 and fall (light blue line in Figure 3(f)) 2022 and a significant positive anomaly of FLOAT climatology compared to SDC one
247 (black line in Figure 2(e) and light blue line in Figure 3(f)). In fall, largest T_a in the SAP were observed in the deep layer (\sim

248 0.69 °C); Table 2, Figure 3(e)). Mean profiles derived from Float Climatology (black line in Figure 2(e) and light blue line in
249 Figure 3(f)) showed positive values compared to SDC one, confirming the warming trend throughout the water column over
250 the past decade. Beyond the impact of the global warming of the Mediterranean Sea, the 2022 MHW leads to an additional
251 heating in the SAP, which is transferred to the deeper layers favoured by dynamical features of this area.

252 This study shows that the effects of the 2022 MHW are felt in all layers of the Mediterranean Sea with vertical heat propagation
253 extending from the surface to ~1500 m depth. In the surface layer, heat penetration and storage are related to the strength of
254 the stratification and/or advection from adjacent regions. In contrast, the transport and the storage of heat in the intermediate
255 and deep layers are closely linked to the dynamics of each area. In the western Mediterranean and western Ionian Sea sectors,
256 heat is mainly stored in the surface layer (shallow MHW depths and stronger stratification) so that this layer is significantly
257 warmer than the climatology even during the following fall. Although deep MHW penetration in these regions is limited to
258 coastal and frontal/eddies zones, it reaches the higher MHW depth estimated during the event. Sectors characterized by specific
259 dynamics conditions (downwelling, convection) quickly distribute the heat in the water column even during the event.
260 Intermediate layers show similar heating both during and after the MHW event, suggesting that heat can be stored here for
261 long periods. The warming signal in the intermediate and deep layers could also be influenced by heat advection from adjacent
262 basins however, we are aware that this topic needs to be studied in more detail in the future. In this context, the use of two
263 climatologies and the cumulative anomaly threshold in the present analysis should have eliminated most of the signal
264 associated with the ocean warming trend and advection therefore, the additional warming registered in spring-summer 2022
265 compared to the FLOAT climatology can be attributed to the effects of the 2022 MHW along the entire water column. Further
266 studies are needed to investigate the effects that this warming may have on the physical and biological oceanic processes with
267 implications on the thermohaline circulation of the entire Mediterranean Sea.

268
269
270
271
272

273 Competing interests. The contact author has declared that neither they nor their co-authors have any competing interests.

274

275 Author contributions. Conceptualization of the study was done by AP, MM and RM. AP and MM prepared the original
276 manuscript. AP, MM, RM, EM, AG, GN, EK and MJ reviewed and edited the manuscript. AP, MM and RM created the
277 methodology. AP, MM, RM and EK created the codes and performed the formal analysis. AP, MM, RM conducted the
278 investigation. AG, AB and MP curated the data. EM was in charge of Argo-Italy infrastructure management and funding
279 acquisition. All authors have read and agreed to the published version of the paper.

280 **References**

281 Argo: Argo float data and metadata from Global Data Assembly Centre (Argo GDAC). SEANOE.
282 <https://doi.org/10.17882/42182>, 2023.

283 Ayoub, N., Le Traon, P.-Y., and De Mey, P.: A description of the Mediterranean surface variable circulation from combined
284 ERS-1 and TOPEX/POSEIDON altimetric data. *J.Mar. Syst.* 18, 3–40, [https://doi.org/10.1016/S0924-7963\(98\)80004-3](https://doi.org/10.1016/S0924-7963(98)80004-3), 1998.

285 Bensoussan, N., Chiggiato, J., Buongiorno Nardelli, B., Pisano, A. and Garrabou, J.: Insights on 2017 marine heat waves in
286 the Mediterranean sea. *J. Oper. Ocean.*, 12 (1), s26–s30, <https://doi.org/10.1080/1755876X.2019.163307>, 2019.

287 Darmaraki, S., Somot, S., Sevault, F. and Nabat, P.: Past variability of Mediterranean Sea marine heatwaves, *Geophys. Res.*
288 *Let.*, 46 (16), 9813–9823, <https://doi.org/10.1029/2019GL082933>, 2019.

289 Dayan, H., McAdam, R., Juza, M., Masina, S. and Speich, S.: Marine heat waves in the Mediterranean Sea: An assessment
290 from the surface to the subsurface to meet national needs. *Front. Mar. Sci.*, <https://doi.org/10.1045138>,
291 1010.3389/fmars.2023.1045138, 2023.

292 Elzahaby, Y. and Schaffer, A.: Observational insight into the subsurface anomalies of marine heatwaves. *Front. Mar. Sci.*,
293 6:745, <https://doi.org/10.3389/fmars.2019.00745>, 2019.

294 Escudier, R., Clementi, E., Cipollone, A., Pistoia, J., Drudi, M., Grandi, A., Lyubartsev, V., Lecci, R., Aydogdu, A., Delrosso,
295 D., Omar, M., Masina, S., Coppini, G. and Pinardi, N.: A High Resolution Reanalysis for the Mediterranean Sea. *Front. Earth*
296 *Sci.*, 9:702285, <https://doi.org/10.3389/feart.2021.702285>, 2021.

297 Falcini, F. and Salusti, E.: Friction and mixing effects on potential vorticity for bottom current crossing a marine strait: an
298 application to the Sicily Channel (central Mediterranean Sea). *Ocean Sci.*, 11, 391–403, [https://doi.org/10.5194/os-11-391-](https://doi.org/10.5194/os-11-391-2015)
299 2015, 2015.

300 Galli, G., Solidoro C., and Lovato T.: Marine heat waves hazard 3D maps and the risk for low motility organisms in a warming
301 Mediterranean Sea. *Front. Mar. Sci.*, 4: 136, <https://doi.org/10.3389/fmars.2017.00136>, 2017.

302 Garrabou, J. et al.: Marine heatwaves drive recurrent mass mortalities in the Mediterranean Sea. *Global Change Biology*,
303 <https://doi.org/10.1111/gcb.16301>, 2022

304 Hobday, A. J., Alexander, L. V., Perkins, S. E., Smale, D. A., Straub, S. C., Oliver, E. C., Benthuisen, J. A., Burrows, M. T.,
305 Donat, G. M., Feng, M., Holbrook, N., J., Moore, P. J., Scannel, H. A., Gupta, A. S. and Wernberg T.: A hierarchical approach
306 to defining marine heatwaves. *Prog. Oceanogr.* 141, 227–238, <https://doi.org/10.1016/j.pocean.2015.12.014>, 2016.

- 307 Ibrahim, O., Mohamed, B., and Nagy, H.: Spatial variability and trends of marine heat waves in the Eastern Mediterranean
308 Sea over 39 years. *J. Mar. Sci. Eng.*, 9 (6), 643, <https://doi.org/10.3390/jmse9060643>, 2021.
- 309 Intergovernmental Panel on Climate Change (IPCC): Summary for Policymakers. In: *Climate Change 2023, Synthesis Report,*
310 *Summary for Policymakers, Core Writing Team, Lee, H. and Romero, J.*, 36,
311 https://www.ipcc.ch/report/ar6/syr/downloads/report/IPCC_AR6_SYR_SPM.pdf, 2023.
- 312 Juza, M., Fernández-Mora, A., and Tintoré, J.: Sub-Regional marine heat waves in the Mediterranean Sea from observations:
313 long-term surface changes, subsurface and coastal responses. *Front. Mar. Sci.* 9, 785771, <https://doi.org/10.3389/fmars.2022.785771>, 2022.
- 315 Kovačević, V., Ursella, L., Gačić, M., Notarstefano, G., Menna, M., Bensi, M., and Poulain, P.-M.: On the Ionian thermohaline
316 properties and circulation in 2010-2013 as measured by Argo floats. *Acta Adriat.*, 56(1): 97 - 114, 2015.
- 317 Kubin, E., Menna, M., Mauri, E., Notarstefano, G., Mieruch, S., and Poulain, P.-M.: Heat content and temperature trends in
318 the Mediterranean Sea as derived from Argo float data. *Front. Mar. Sci.* 10, 1271638,
319 <https://doi.org/10.3389/fmars.2023.1271638>, 2023
- 320 Malanotte-Rizzoli, P., Manca, B. B., Ribera D'Alcalà, M., Theocharis, A., Bergamasco, A., Bregant, D., Budillon, G.,
321 Civitarese, G., Georgopoulos, D., Michelato A., Sansone, E., Scarazzato, P., Souvermezoglou, E.: A synthesis of
322 the Ionian Sea hydrography, circulation and water masses pathways during POEM-Phase I. *Progr. Oceanogr.*, 39, 153–204,
323 [https://doi.org/10.1016/S0079-6611\(97\)00013-X](https://doi.org/10.1016/S0079-6611(97)00013-X), 1997.
- 324 Menna, M., Suarez, N. R., Civitarese, G., Gačić, M., Rubino, A., and Poulain, P. M.: Decadal variations of circulation in the
325 Central Mediterranean and its interactions with mesoscale gyres. *Deep Sea Res. II*, 164, 14-24,
326 <https://doi.org/10.1016/j.dsr2.2019.02.004>, 2019a.
- 327 Menna, M., Poulain, P. M., Ciani, D., Doglioli, A., Notarstefano, G., Gerin, R., Rio, M. H. Santoleri, R., Gauci, A. and Drago,
328 A.: New Insights of the Sicily Channel and Southern Tyrrhenian Sea Variability. *Water*, 11, 1355,
329 <https://doi.org/10.3390/w11071355>, 2019b.
- 330 Menna, M., Gerin, R., Notarstefano, G., Mauri, E., Bussani, A., Pacciaroni, M., and Poulain, P. M.: On the circulation and
331 thermohaline properties of the Eastern Mediterranean Sea. *Fron. Mar. Sci.*, 8, 671469,
332 <https://doi.org/10.3389/fmars.2021.6714692>, 2021.
- 333 Menna, M., Martellucci, R., Notarstefano, G., Mauri, E., Gerin, R., Pacciaroni, M., Bussani, A., Pirro, A., Poulain, P. M.:
334 Record-breaking high salinity in the South Adriatic Pit in 2020. *J. Oper. Oceanogr.*, s199-s205,
335 <https://doi.org/10.1080/1755876X.2022.2095169>, 2022.
- 336 Mihanović, H., Vilibić, I., Šepić, J., Matic, F., Ljubešić, Z., Mauri, E., Gerin, R.: Observation, preconditioning and recurrence
337 of exceptionally high salinities in the Adriatic Sea. *Front. Mar. Sci.*, 8:834. <https://doi.org/10.3389/fmars.2021.672210>, 2021.
- 338 Molcard, A., Gervasio, L., Gria, A., Gasparini, G. P., Mortier, L., Ozgokmen, T. M.: Numerical investigation of the Sicily
339 Channel dynamics: density currents and water mass advection. *J. Mar. Syst.*, 36, 219–238, [https://doi.org/10.1016/S0924-7963\(02\)00188-4](https://doi.org/10.1016/S0924-7963(02)00188-4), 2002.
- 341 Mkhinini, N., Coimbra, A. L. S., Stegner, A., Arsouze, T., Taupier-Letage, I., and Beranger, K.: Long-lived mesoscale eddies
342 in the Eastern Mediterranean Sea: analysis of 20 years of AVISO geostrophic velocities. *J. Geophys. Res. Oceans* 119, 8603–
343 8626, <https://doi.org/10.1002/2014JC010176>, 2014.

344 Oliver, E. C., Donat, M. G., Burrows, M. T., Moore, P. J., Smale, D. A., Alexander, L. V., Benthuisen, J. A., Feng, M., Gupta,
345 A. S., Hobday, A. J., Holbrook, N. J., Perkins-Kirkpatrick, S. E., Scannell, H. E., Straub, S. C. and Wernberg, T.: Longer and
346 more frequent marine heatwaves over the past century. *Nat. Commun.*, 9:1324, <https://doi.org/10.1038/s41467-018-03732-9>,
347 2018.

348 Pinardi, N., Zavatarelli, M., Adani, M., Coppini, G., Fratianni, C., Oddo, P., Simoncelli, S., Tonani, M., Lyubartsev, V.:
349 Mediterranean Sea large-scale low-frequency ocean variability and water mass formation rates from 1987 to 2007: a
350 retrospective analysis. *Prog. Oceanogr.* 132, 318–332, <https://doi.org/10.1016/j.pocean.2013.11.003>, 2015.

351 Pirro, A., Mauri, E., Gerin, R., Martellucci, R., Zuppelli, P. and Poulain, P. M.: New insights on the formation and breaking
352 mechanism of convective cyclonic cones in the South Adriatic Pit during winter 2018. *J. Phys. Oceanogr.*, 52(9), 2049–2068,
353 <https://doi.org/10.1175/JPO-D-21-0108.1>, 2022.

354 Poulain, P. M., Menna, M., and Mauri, E.: Surface geostrophic circulation of the Mediterranean Sea derived from drifter and
355 satellite altimeter data. *J. Phys. Oceanogr.*, 42(6), 973–990, <https://doi.org/10.1175/JPO-D-11-0159.1>, 2012.

356 Poulain, P. M., Bussani, A., Gerin, R., Jungwirth, R., Mauri, E., Menna, M. and Notarstefano, G.: Mediterranean surface
357 currents measured with drifters: From basin to subinertial scales. *Oceanography* 26 (1), 38–47,
358 <https://doi.org/10.5670/oceanog.2013.03>, 2013.

359 Poulain, P. M., Centurioni, L., Özgökmen, T., Tarry, D., Pascual, A., Ruiz, S., Mauri, E., Menna, M. and Notarstefano, G.: On
360 the structure and kinematics of an Algerian Eddy in the southwestern Mediterranean Sea. *Rem. Sens.*, 13(15), 3039,
361 <https://doi.org/10.3390/rs13153039>, 2021.

362 Pastor, F. and Khodayar, S.: Marine heat waves: Characterizing a major climate impact in the Mediterranean. *Sci. Tot. Env.*,
363 861, 160621, <https://doi.org/10.1016/j.scitotenv.2022.160621>, 2022.

364 Scannell, H. A., Johnson, G. C., Thompson, L., Lyman, J. M., and Riser, S. C.: Subsurface evolution and persistence of marine
365 heatwaves in the Northeast Pacific. *Geophys. Res. Lett.*, 47, e2020GL090548, <https://doi.org/10.1029/2020GL090548>, 2020.

366 Schroeder, K., Chiggiato, J., Josey, S.A., Borghini, M., Aracri, S., Sparnocchia, S.: Rapid response to climate change in a
367 marginal sea. *Sci. Rep.*, 7, 4065, <https://doi.org/10.1038/s41598-017-04455-5>, 2017.

368 Shijian H., S., Li, S., Zhang, Y., Guan, C., Du, Y., Feng, M., Anodo, K., Wang, F., Schiller, A. and Hu, D.: Observed strong
369 subsurface marine heatwaves in the tropical western Pacific Ocean. *Env. Res. Lett.*, 16(10), 104024,16 104024,
370 <https://doi.org/10.1088/1748-9326/ac26f2>, 2021.

371 Von Schuckmann, K., Palmer, M. D., Trenberth, K. E., Cazenave, A., Chambers, D., Champollion, N., Hansen, J., Josey, S.
372 A., Loeb, N., Mathieu, P. P., Meyssignac, B. and Wild, M.: An imperative to monitor earth’s energy imbalance. *Nat. Clim.*
373 *Change*, 6 (2), 138–144, doi:10.1038/nclimate2876, 2016.

374 Wernberg, T., Smale, D. A., Tuya, F., Thomsen, M. S., Langlois, T. J., De Bettignies, T., Bennet, S. and Rousseaux, C. S.: An
375 extreme climatic event alters marine ecosystem structure in a global biodiversity hotspot. *Nat. Clim. Change*, 3, 78–82,
376 <https://doi.org/10.1038/nclimate1627>, 2013.

377 Wong, A. P., Wijffels, S. E., Riser, S. C., Pouliquen, S., Hosoda, S., Roemmich, D., et al.: Argo Data 1999–2019: Two Million
378 Temperature-Salinity Profiles and Subsurface Velocity Observations From a Global Array of Profiling Floats. *Front. Mar. Sci.*,
379 7(700), <https://doi.org/10.3389/fmars.2020.00700>, 2020.

380

381 **References for Table 1**

382 Product ref no.1

383 EU Copernicus Marine Service Product: Mediterranean Sea- In-Situ Near Real Time Observations, Mercator Ocean
384 International [data set], <https://doi.org/10.48670/moi-00044>, 2022.

385 H. Wehde, K. V. Schuckmann, S. Pouliquen, A. Grouazel, T Bartolome, J Tintore, M. De Alfonso Alonso-Munoyerro, T.
386 Carval, V. Racapé and the INSTAC team: EU Copernicus Marine Service Quality Information Document for Mediterranean
387 Sea- In-Situ Near Real Time Observations, INSITU_MED_PHYBGCWAV_DISCRETE_MYNRT_013_035, Issue 2.2,
388 Mercator Ocean International, [https://catalogue.marine.copernicus.eu/documents/QUID/CMEMS-INS-QUID-013-030-
389 036.pdf](https://catalogue.marine.copernicus.eu/documents/QUID/CMEMS-INS-QUID-013-030-036.pdf), last access: 19 May 2023, 2022.

390 In Situ TAC partners: EU Copernicus Marine Service Product User Manual for Mediterranean Sea- In-Situ Near Real Time
391 Observations, INSITU_MED_PHYBGCWAV_DISCRETE_MYNRT_013_035, Issue 1.14, Mercator Ocean International,
392 <https://catalogue.marine.copernicus.eu/documents/PUM/CMEMS-INS-PUM-013-030-036.pdf>, last access: 19 May 2023,
393 2022.

394 Product ref no.2

395 EU Copernicus Marine Service Product: Mediterranean Sea Physics Reanalysis, Mercator Ocean International [data set],
396 https://doi.org/10.25423/CMCC/MEDSEA_MULTIYEAR_PHY_006_004_E3R1I, 2022.

397 R. Escudier, E. Clementi, T. Nigam, A. Aydogdu, E. Fini, J. Pistoia, A. Grandi, P. Miraglio: EU Copernicus Marine Service
398 Quality Information Document for Mediterranean Sea Physics Reanalysis, MEDSEA_MULTIYEAR_PHY_006_004, Issue
399 2.3, Mercator Ocean International, [https://catalogue.marine.copernicus.eu/documents/QUID/CMEMS-MED-QUID-006-
400 004.pdf](https://catalogue.marine.copernicus.eu/documents/QUID/CMEMS-MED-QUID-006-004.pdf), last access: 19 May 2023, 2022.

401 Rita Lecci, Massimiliano Drudi, Alessandro Grandi, Sergio Creti, Emanuela Clementi: EU Copernicus Marine Service Product
402 User Manual for For Mediterranean Sea Physics Reanalysis, MEDSEA_MULTIYEAR_PHY_006_004, Issue 2.3, Mercator
403 Ocean International, <https://catalogue.marine.copernicus.eu/documents/PUM/CMEMS-MED-PUM-006-004.pdf>, last access:
404 19 May 2023, 2022.

405 Product ref no.3

406 EU Copernicus Marine Service Product: European Seas Gridded L 4 Sea Surface Heights And Derived Variables Nrt, Mercator
407 Ocean International [data set], <https://doi.org/10.48670/moi-00142>, 2023.

408 M-I Pujol, G. Taburet and SL-TAC team.: EU Copernicus Marine Service Quality Information Document for European Seas
409 Gridded L 4 Sea Surface Heights And Derived Variables Nrt,
410 SEALEVEL_EUR_PHY_L4_NRT_OBSERVATIONS_008_060, Issue 8.2, Mercator Ocean International,
411 <https://catalogue.marine.copernicus.eu/documents/QUID/CMEMS-SL-QUID-008-032-068.pdf>, last access: 19 May 2023,
412 2023.

413 M-I Pujol: EU Copernicus Marine Service Product User Manual for European Seas Gridded L 4 Sea Surface Heights And
414 Derived Variables Nrt, SEALEVEL_EUR_PHY_L4_NRT_OBSERVATIONS_008_060, Issue 7.0, Mercator Ocean
415 International, <https://catalogue.marine.copernicus.eu/documents/PUM/CMEMS-SL-PUM-008-032-068.pdf>, last access: 19
416 May 2023, 2022.

417 Product ref no.4

418 S. Simoncelli , P. Oliveri , G. Mattia. SeaDataCloud Mediterranean Sea - V2 Temperature and Salinity Climatology [dataset].
419 <http://dx.doi.org/10.12770/3f8eaace-9f9b-4b1b-a7a4-9c55270e205a> [Accessed on 19 May 2023]

420 Simoncelli Simona, Oliveri Paolo, Mattia Gelsomina, Myroshnychenko Volodymyr, Barth Alexander, Troupin Charles (2020).
421 SeaDataCloud Temperature and Salinity Climatology for the Mediterranean Sea (Version 2). Product Information Document
422 (PIDoc). <https://doi.org/10.13155/77514>

423

424

425